Applied Catalysis B: Environmental 341 (2024) 123333

Contents lists available at ScienceDirect

Applied Catalysis B: Environmental

journal homepage: www.elsevier.com/locate/apcatb

Regeneration of a sulfur-poisoned selective catalytic reduction catalyst at ambient conditions

Hwangho Lee [a], Inhak Song [b], Se Won Jeon [a], Keon Ha Hwang [a], Do Heui Kim [a,*]

[a] Department School of Chemical and Biological Engineering, Institute of Chemical Processes, Seoul National University, Seoul 08826, Republic of Korea
[b] Department of Energy Environment Policy and Technology, Graduate School of Energy and Environment (KU-KIST Green School), Korea University, Seoul 02841, Republic of Korea

ARTICLE INFO

Keywords:
NH_3-SCR
Physical mixed catalyst
Sulfur poisoning
Ammonium bisulfate
Catalytic regeneration

ABSTRACT

Despite the high sulfur resistance of vanadia-titania catalysts with physically mixed zeolite in the selective catalytic reduction of NO_x (SCR), their regeneration is still challenging because it typically requires a large amount of energy or hazardous chemicals. This paper proposes an innovative regeneration strategy for prolonging the lifetime of the sulfur-poisoned catalyst. Our spectroscopic results revealed that the adsorbed water in the catalyst dissolves the deactivating material, ammonium bisulfate (ABS). We developed a regeneration protocol based on this finding, which was facilitated by dissolution of ABS in water adsorbed on the catalyst during the exposure to humid air at ambient temperature. The superior hydrophilic nature of zeolite resulted in a different water content between two physically mixed domains, promoting ABS migration from the vanadia active sites to zeolite and thus recovering the catalytic activity. This strategy is beneficial for the development of energy-efficient and environmentally friendly SCR systems.

1. Introduction

Fossil fuels still account for more than 80% of the global energy production despite several attempts to address the issues associated with the increasing global energy consumption [1,2]. Nitrogen oxide (NO_x) emissions, which are inevitably produced by fuel combustion, have been a cause of concern because of their role as primary pollutants in photochemical smog and their contribution to particulate matters [3,4]. Consequently, NO_x emission regulations, such as EURO 6, TIER III, and CHINA 5, are becoming more stringent in many countries [5], and post-treatment systems have been implemented in various industrial fields to abide by these regulations [6].

The selective catalytic reduction of NO_x with NH_3 (NH_3-SCR) is the most powerful NO_x removal method that converts NO_x into harmless N_2 using ammonia as a reductant [7,8]. Vanadia-based metal oxides and Cu-ion-exchanged zeolites have been widely employed as catalysts in the NH_3-SCR reaction owing to their excellent NO_x removal ability [9–17]. Despite their excellent performance, their industrial application is still challenging due to several issues including the inability to remove NO_x at temperatures below 250 °C [18,19]. Since the SCR reactor is positioned at the tail end of the post-treatment system, a gas temperature generally reaches to below 250 °C. This temperature is lower than the operating temperature of conventional SCR catalysts [20,21]. Therefore, gas reheating is required for SCR operation, and a considerable amount of additional energy is thus consumed. Several studies have reported the development of low-temperature SCR catalysts [22–27].

However, the vulnerability of these catalysts to SO_2 poisoning has restricted their industrial application. Despite the use of low-sulfur fuels and desulfurization processes, exhaust gases still contain a few parts per million (ppm) of SO_2, especially in stationary plants [2], and the presence of such trace amounts of sulfur can poison the active sites of these catalysts by forming inactive metal-sulfate species [28]. This deactivation severely degrades the catalytic performance, requiring high temperatures above 600 °C for catalyst regeneration. Although vanadia-based catalysts are relatively resistant to sulfur, they are deactivated at low temperatures owing to the formation of liquid ammonium bisulfate (ABS), which blocks the active vanadia sites [23]. Consequently, the incompatibility between sulfur resistance and low-temperature activity remains a challenging issue in NO_x removal [29].

Recently, Song et al. and Jeon et al. reported a catalyst exhibiting a high SCR activity and high sulfur resistance at low temperatures [30–32]. They reported that the introduction of physically mixed zeolite into vanadia-based catalysts prevents blockage of the active sites of the

* Corresponding author.
E-mail address: dohkim@snu.ac.kr (D.H. Kim).

https://doi.org/10.1016/j.apcatb.2023.123333
Received 8 August 2023; Received in revised form 17 September 2023; Accepted 22 September 2023
Available online 25 September 2023

catalyst by inducing ABS migration from the vanadia sites into the zeolite [33]. The developed catalyst exhibited high sulfur resistance and was regenerable and reusable after thermal treatment at temperatures above 350 °C. However, a large amount of energy was required to heat the reactor during thermal treatment, which is a conventional regeneration process. Therefore, in terms of long-term usage, repeated regeneration inevitably incurs high energy costs and causes emission of greenhouse gases, which is a critical industrial issue. A few other strategies have been proposed for the regeneration of sulfur-poisoned catalysts; however, these require the use of toxic chemicals, such as NO_2 and nitric acid, which is highly undesirable and impractical [34–36]. Despite their significant impact on the environment, little effort has been devoted to the development of an effective and ecological method for regenerating deactivated catalysts. This study investigated the physicochemical properties of ABS on a vanadia catalyst with physically mixed zeolite using various spectroscopic techniques to elucidate its behavior on the catalyst surface. A novel regeneration strategy was then developed to recover the SCR activity of a degraded catalyst without additional energy input or the use of chemicals.

2. Experimental

2.1. Synthesis of the catalyst and its physical mixing with zeolite

The V_2O_5-WO_3-TiO_2 (VWTi) catalyst was synthesized using the wet impregnation method. A DT-52 TiO_2 support (WTi, 7.7 wt% of tungsten, CRYSTAL) was added into the vanadium precursor solution, which was prepared by dissolving ammonium metavanadate (Sigma Aldrich) in an oxalic acid solution (Sigma Aldrich). The solution containing the DT-52 support was stirred for 30 min and dehydrated using a rotary evaporator. The catalyst was completely dried overnight in a forced-convection oven at 105 °C and calcined at 500 °C for 4 h. The composition of the resulting VWTi material was analyzed using inductively coupled plasma atomic emission spectroscopy (ICP-AES). The prepared VWTi catalyst was physically mixed with an NH_4^+-Y zeolite (Si/Al_2 =12, Alfa Aesar) in a 2:1 mass ratio, and the mixture was annotated as VWTi+Z. To prepare the ABS-impregnated VWTi, an ABS salt (Sigma Aldrich) was dissolved in deionized (DI) water, and the solution was used to impregnate the VWTi catalyst using the incipient wetness impregnation method. Subsequently, the sample was dried in a forced-convection oven at 105 °C. The samples were annotated as ABS(2)/VWTi (2 wt% of ABS) or ABS(10)/VWTi (10 wt% of ABS) depending on the ABS loading. The same method was employed to prepare ABS-impregnated Y zeolite (ABS/Z). The hydrophobic Y zeolite was synthesized by functionalizing the zeolite surface with OTS (Sigma Aldrich) as a silylating agent. Briefly, the Y zeolite (1 g, Si/Al_2 =12) was dispersed in toluene (20 mL) by sonication. The zeolite suspension was then added to a mixture of toluene (50 mL) and OTS (0.59 mL). The solution was stirred for 24 h at 25 °C and filtered using ethanol (1 L). The filtered samples were dried overnight in a convection oven at 105 °C (denoted as OTS-Z).

2.2. Catalyst characterization

ICP-AES analyses were performed on an OPTIMA 8300 (Perkin-Elmer) spectrometer to measure the loadings of vanadium and tungsten in VWTi. The deposited sulfur content was measured by elemental analysis using a Flash2000 analyzer (Thermo Fisher Scientific). TEM images were obtained using a JEM-ARM2000F microscope at 200 kV with a spherical aberration correction. TEM samples were prepared by making catalyst as suspension in acetone solvent in which ABS is not soluble. The suspension was dropped onto a 200-mesh carbon-coated copper grid and dried at 105 °C. Line-EDS images were obtained in the scanning transmission electron microscopy (STEM) mode. Mass spectrometry was performed on a HIDEN Analytical QGA device using a secondary electron multiplier detector. DRIFTS analyses were conducted in a diffuse reflectance cell (Praying Mantis, Harrick) using a Fourier-transform infrared (FTIR) spectrometer (IS-50, Thermo Fisher Scientific). Additionally, outlet gas analyses were performed using FTIR spectroscopy (Nicolet6700, Thermo Fisher Scientific) with a 2 m gas cell (Gemini, International Crystal Laboratories). A mercury-cadmium-telluride (MCT) type detector was used for all FTIR analyses. TGA was performed using an SDT Q600 instrument (TA Instruments) under a 20% O_2/N_2 atmosphere. The adsorbed water content was measured using a dynamic vapor sorption-intrinsic analyzer (Micromeritics) at 40 °C.

2.3. NH_3-SCR reaction

The NH_3-SCR reactivity and SO_2 aging data were measured in a down-flow 1/4" internal diameter tubular quartz reactor. All samples were sieved into 180–250-μm particles and pelletized to prevent pressure drop. The reactions were conducted with 500 ppm NO (5000 ppm in N_2, Deokyang Co., Ltd.), 600 ppm NH_3 (5000 ppm in N_2, Deokyang Co., Ltd.), 10% O_2 (99.995%, Daesung Industrial Gases Co., Ltd.), 5% CO_2 (99.999%, KS gas Co., Ltd.), 10% H_2O (DI, introduced from PURELAB Chorus, ELGA), 30 or 100 ppm SO_2 (when used, 1000 ppm in N_2, Deokyang Co., Ltd.), and balance N_2 (99.999%, Daesung Industrial Gases Co., Ltd.). The space velocity (SV) was 150,000 mL/h·g_{cat} based on the mass of VWTi catalyst. For the physically mixed samples, the GHSV was set based on the weight of VWTi. NO_x concentrations were measured using an NO_x chemiluminescence analyzer (42i High level, Thermo Scientific), and NO_x conversions were calculated according to Eq. (1).

$$NO_x \quad \text{conversion} \quad (\%) = \frac{[NO_x]_{in} - [NO_x]_{out}}{[NO_x]_{in}} \times 100 \tag{1}$$

To test the resistance of the catalysts to SO_2 poisoning, the samples were treated for 22 h under NH_3-SCR conditions with 30 or 100 ppm SO_2 and 220 °C. The rate of NO_x consumption was calculated using Eq. (2), and $\ln(-r_{NO})$ vs. 1/T was plotted to obtain the Arrhenius plots.

$$-r_{NOx}\left(mol_{NOx}\ s^{-1}\right) = \frac{\left(C_{NOx,in} - C_{NOx,out}\right)}{1000000} V_{total}\left(\frac{P}{RT}\right) \tag{2}$$

Where, C is the NO_x concentration (ppm) measured by the NO_x analyzer, V_{total} is the total volumetric flow rate (0.2 L/min), P is 1 atm, T is the ambient temperature, and R is the gas constant.

3. Results and discussion

3.1. Imaging of ABS migration in the physically mixed catalyst

After investigating the improvement in sulfur resistance of a vanadia-tungsta-titania (VWTi) catalyst with physically mixed zeolite, our group proposed an optimized VWTi+Z catalyst in which the Y zeolite (Si/Al_2 = 12) is used as the physically mixed zeolite (Z) [30]. The results (Fig. S1) revealed that the VWTi+Z catalyst retained the surface area, crystal structure, and reduction properties of its components, VWTi and the Y zeolite, which can be attributed to the mixing of the two materials by physical grinding, which barely changes the properties of the components. Consequently, the VWTi and VWTi+Z catalysts demonstrated almost identical SCR activities (Fig. S2). The change in the SCR activities of the VWTi+Z and conventional VWTi catalysts in the presence of 30 ppm SO_2 was investigated (Fig. S3a), and the results revealed that the VWTi+Z catalyst had a significantly higher sulfur resistance. After the SCR reaction in the presence of 30 ppm SO_2, the elemental distribution in the aged catalyst was observed by transmission electron microscopy (TEM) and electron dispersive spectroscopy (EDS), which revealed the presence of the vast majority of sulfur species in the zeolite region and its absence in the VWTi region. Since the accumulation of sulfur species is caused by ABS formation, which proceeds by the oxidation of SO_2 to SO_3 on vanadia, and since the Y zeolite is almost inert in both SO_2 adsorption

and oxidation, this distribution in the physically mixed catalyst can be attributed to the migration of the sulfur species (i.e., ABS) from VWTi to the zeolite [19,30,37]. To confirm this migration, VWTi was impregnated with ABS and physically mixed with the zeolite (ABS(x)/VWTi+Z, where x is the weight percent of ABS relative to VWTi). After exposing the ABS(2)/VWTi and ABS(2)/VWTi+Z samples to the standard SCR conditions at 220 °C, the location of sulfur on the samples was visualized by TEM-EDS. The zeolite (Z) and VWTi were clearly distinct in the TEM images (bright region with large particles of size ~300 nm for the zeolite and a dark region with small particles of size ~10 nm for VWTi) and the line-EDS signal (silicon for zeolite and titanium for VWTi) (Fig. 1a-d). These data confirmed that the ABS-impregnated sulfur species are localized at the zeolite rather than VWTi, even though they were initially impregnated on VWTi. It was thus concluded that the ABS species deposited on the catalyst during SO_2 aging can migrate from VWTi to the zeolite in the physically mixed VWTi+Z catalyst.

As ABS exists as liquid at 220 °C, a physical channel is required between the zeolite and VWTi to enable its migration. Thus, it was hypothesized that physical contact between the zeolite and VWTi can facilitate this migration and that their interfaces can provide a migration pathway. To investigate the significance of this physical contact, a physically mixed catalyst with minimal physical contact was fabricated (VWTi+Z PM L; physically mixed loosely). The VWTi+Z PM L catalyst was prepared by mixing the Y zeolite and VWTi catalyst, which were sieved into 180 μm granules before being mixed. Because vortex mixing was performed without grinding the particles, they were macroscopically mixed but exhibited little physical interaction microscopically. ABS (2 wt%) was impregnated on VWTi before physical mixing to prepare the ABS(2)/VWTi+Z and ABS(2)/VWTi+Z PM L catalysts. In a physically mixed catalyst, the Y zeolite barely influences the intrinsic SCR activity of VWTi; therefore, the extent of physical contact is the only difference between these catalysts (Fig. S2). The SCR activities of VWTi, ABS(2)/VWTi+Z, and ABS(2)/VWTi+Z PM L catalysts were measured at various temperatures, and the data are presented as an Arrhenius plot (Fig. S4). Regardless of the ABS impregnation, the Arrhenius plots of the three catalysts were almost identical at temperatures below the melting point of ABS at approximately 160 °C, demonstrating that ABS has a negligible effect on the activity of vanadia sites when it exists as a solid, since the physical deactivation is induced by liquid ABS, which is highly adhesive and blocks the active sites [30,38]. At temperatures above the melting point of ABS (>200 °C), deactivation by ABS was observed in ABS(2)/VWTi+Z PM L, whose plot displayed lower reaction rates than did that of pristine VWTi. The Arrhenius plots revealed that deactivation reduces the pre-exponential factor without changing the activation energy (~54 kJ/mol). These results strongly indicate that deposited ABS does not chemically deteriorate the active sites but only physically blocks them [38,39]. Although the same amount of ABS was impregnated on vanadia, deactivation was not observed for the ABS (2)/VWTi+Z sample with nearly the same activation energy and pre-exponential factor. Considering the absence of sulfur in the vanadia sites of this catalyst (Fig. 1c, d), it was concluded that the physically mixed zeolite protects the VWTi catalyst by facilitating the migration of the ABS molecules initially formed on the VWTi toward the Y zeolite.

Subsequently, the ABS migration process was spectroscopically monitored by in situ diffuse reflectance infrared Fourier transform spectroscopy (DRIFTS). First, the differences in the vibrational frequency of the impregnated ABS in the VWTi and Y zeolites was investigated. A larger amount of ABS (10 wt%) was impregnated (ABS(10)/VWTi and ABS(10)/Z) to clearly verify these differences. The sulfur species of ABS showed IR absorption peaks in the wavenumber range of 1350–1200 cm^{-1}, attributed to the S═O stretching mode in the bisulfate ion (HSO_4). These peaks were observed at 1260–1250 and 1285–1270 cm^{-1} for the VWTi and Y zeolites, respectively (Fig. S5) [34, 39]. However, the IR peaks of VWTi remained almost unchanged regardless of the temperature. The IR absorption peak of sulfate on the zeolite shifted to a lower wavenumber (from 1290 to 1270 cm^{-1}) as the temperature increased but remained distinct from that of the sulfate on VWTi (1255 cm^{-1}). Therefore, these IR peaks can be used as fingerprints to verify the location of ABS, and thus, the location of the bisulfate species in the physically mixed catalyst can be identified. Based on these

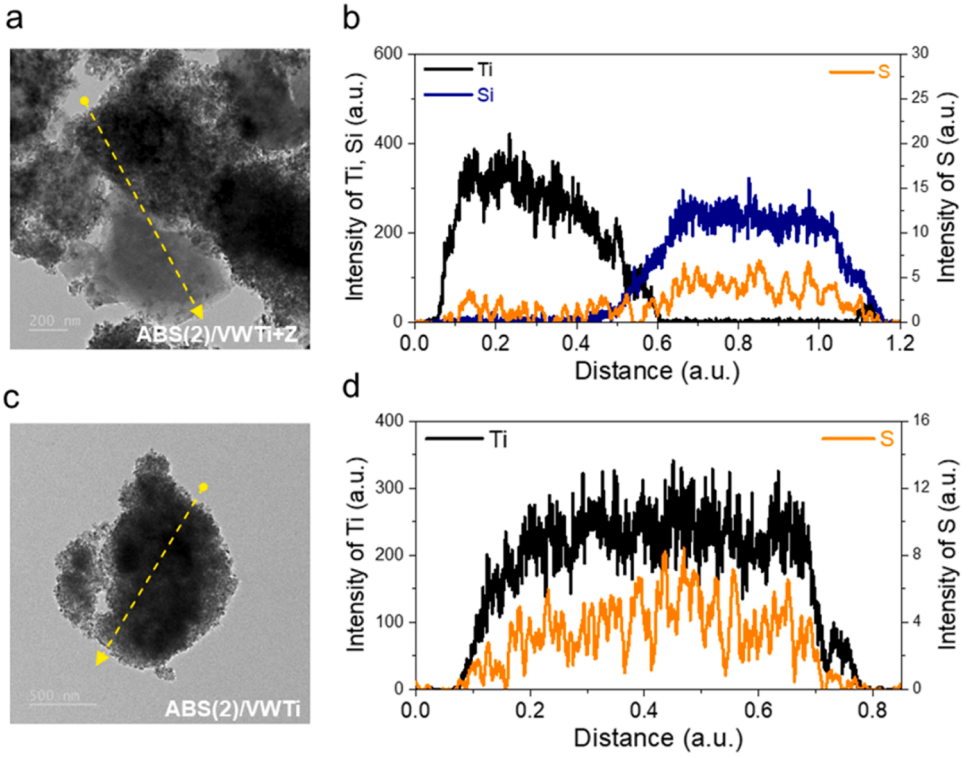

Fig. 1. TEM images and EDX profiles of ABS-impregnated catalysts. (a, b) Images and profiles of ABS(2)/VWTi, respectively. (c, d) Images and profiles of ABS(2)/VWTi+Z, respectively. The EDX profiles show the intensity of each atom (Ti, V, and Si) in the yellow line.

fingerprints, the change in the bisulfate IR peak of the ABS(10)/VWTi+Z PM catalyst was investigated in the temperature range of 100–250 °C (Fig. 2a, b).

The IR peak corresponding to the bisulfate species in the physically mixed catalyst was initially observed at 1255 cm^{-1}, since ABS was impregnated onto VWTi before the physical mixing with the Y zeolite. This peak, which is a characteristic band of the bisulfate species on the Y zeolite, gradually shifted to 1273 cm^{-1} as the temperature increased from 100 to 250 °C (Figs. 2(A) and S5). Additionally, the peak intensity of the bisulfate increased to almost twice the intensity of the initial peak, thus exhibiting the same trend as the peak shift (Fig. 2b). These trends were not observed in the spectra for ABS on VWTi, which exhibited the same peak position and intensity at 100 and 250 °C (Fig. S5). Therefore, these spectroscopic changes exhibited by the bisulfate species represent the migration of ABS from VWTi to the Y zeolite with an increase in the temperature. The profile shown in Fig. 2b illustrates the change in the bisulfate peak during ABS migration. At 178 °C, which is close to the melting point of ABS, the intensity and position of the IR peak changed dramatically, thus indicating the migration of ABS to the Y zeolite upon its transformation into the liquid phase. Hence, a physical channel is essential for this migration. The migration of liquid ABS is a unidirectional movement from VWTi to the Y zeolite owing to the ABS stabilization effect of the Brønsted acid sites and the pore structure of the Y zeolite [30,31]. To confirm this, the same experiment was performed with VWTi+ABS(10)/Z PM, in which ABS was initially impregnated on the Y zeolite rather than on VWTi (Fig. 2c, d). Upon increasing the temperature, the infrared peak at 1255 cm^{-1}, which is the fingerprint for ABS on VWTi, was not observed, thus indicating that the ABS on the Y zeolite did not migrate toward VWTi. This clearly verifies that ABS migration is not a simple diffusion process induced by a concentration gradient but a unidirectional mass transfer process owing to a specific driving force. Based on the results of our previous study, strong electrostatic interaction between ABS and the framework aluminum site in zeolite contributes to molecular migration [30].

3.2. Decomposition behavior of ammonium bisulfate

To gain further insights into the ABS properties, the decomposition behavior of the deposited ABS in the SO_2-poisoned VWTi and VWTi+Z catalysts was investigated via temperature-programmed desorption (TPD) analysis under different gas conditions (N_2 and 10% O_2/N_2). The decomposition profile (Fig. 3a, c), which is a typical ABS decomposition profile, reveals that the ABS deposited on the VWTi catalyst mainly decomposes into NH_3 and SO_2 under a N_2 atmosphere at 350 and 450 °C. The desorption peak of NH_3 in VWTi+Z was observed at a higher temperature (390 °C) because the Y zeolite contains stronger Brønsted acid sites for NH_3 adsorption [40,41]. The SO_2 decomposition peak was observed with an asymmetric peak shape at a temperature similar to that of VWTi. Although the SO_2-poisoned VWTi+Z catalyst contained almost the same amount of sulfur as did the SO_2-poisoned VWTi catalyst, the SO_2 decomposition peak was significantly smaller (Fig. 3c, d and Table S1). This phenomenon can be attributed to the formation of aluminum sulfate species in the VWTi+Z catalyst, which decomposes at a considerably higher temperature (approximately 800 °C) [30]. The strong interaction between the sulfate and the aluminum sites in the zeolite results in the formation of aluminum sulfate species, which partially hinders the ABS decomposition.

By contrast, the profiles of the decomposition of deposited sulfur species under oxidative conditions (10% O_2/N_2) were completely different, where gas-phase SO_2 was not observed in the range of 1400–1300 cm^{-1} (Fig. 4a, b). Instead, broad IR peaks were observed near 1430 and 1055 cm^{-1}, attributed to the aerosol-like species of ammonium sulfate (AS) and ABS, respectively [42,43]. The presence of the aerosol band and absence of the gas phase SO_2 band indicated that the deposited sulfur species were desorbed as an ammonium salt complex under oxidative condition rather than as SO_2 gas, a decomposed form. This different decomposition behavior was investigated under N_2 and O_2/N_2 conditions using DRIFTS. The spectra of ABS impregnated on VWTi displayed IR bands at 1430 and 1250 cm^{-1} at 100 °C, attributed to

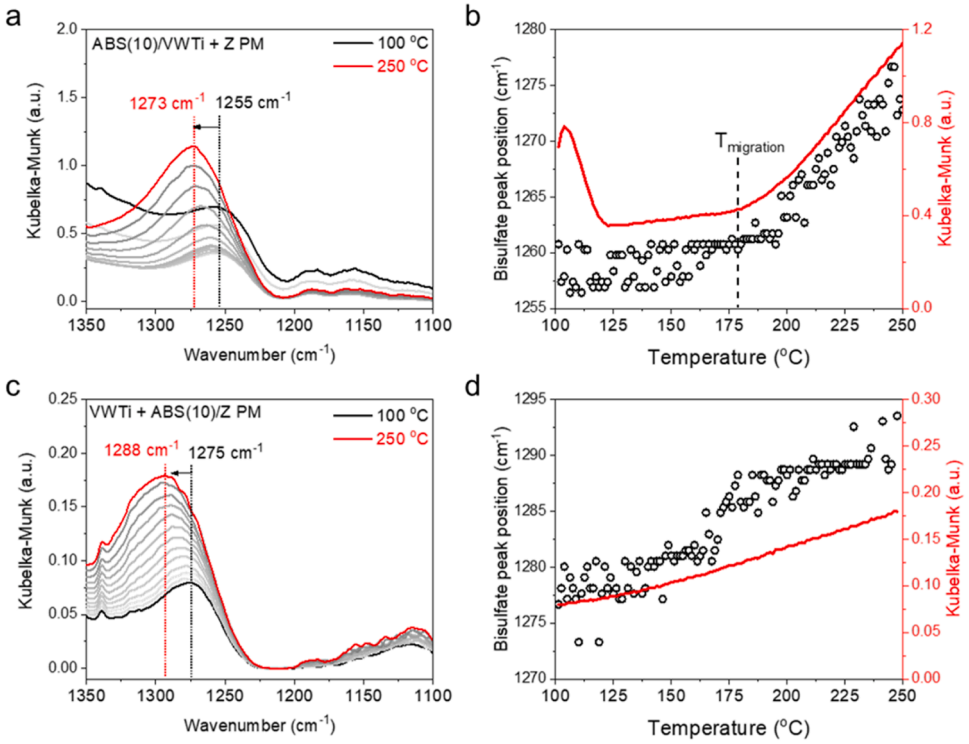

Fig. 2. Time-resolved DRIFT spectra of ABS-impregnated catalysts. (a, b) Spectra and peak profiles of ABS(10)/VWTi, respectively. (c, d) Spectra and peak profiles of ABS(10)/VWTi+Z, respectively. These spectra were obtained while increasing the temperature from 100° to 250°C. The peak profiles show the peak location (left y axis) and intensity (right y axis) of the bisulfate infrared band. $T_{migration}$ in B indicates the temperature at which the ABS migration began.

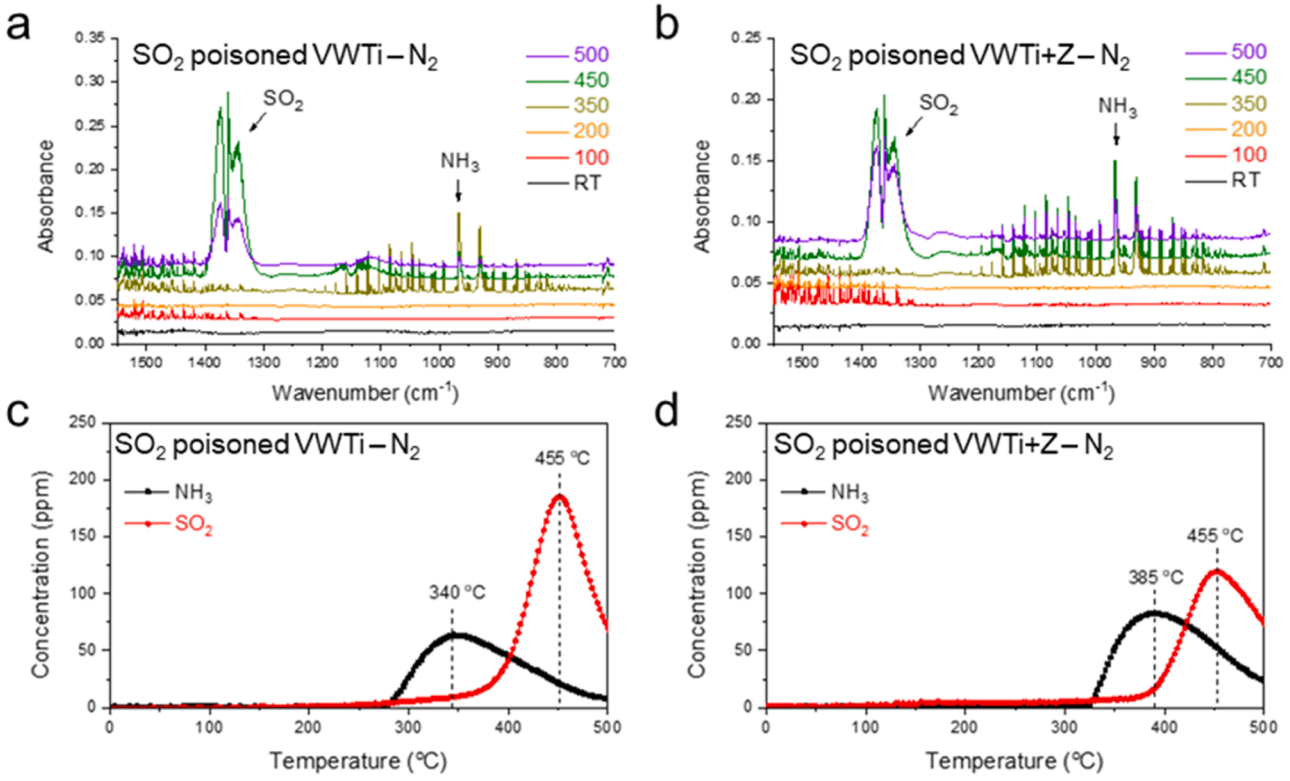

Fig. 3. Temperature-programmed decomposition-infrared spectroscopy results of sulfur-poisoned catalysts under nitrogen. (a, b) Raw infrared spectra and (c, d) Concentration profiles of the gas species from sulfur poisoned VWTi and VWTi+Z catalysts, respectively during the decomposition under N_2 conditions.

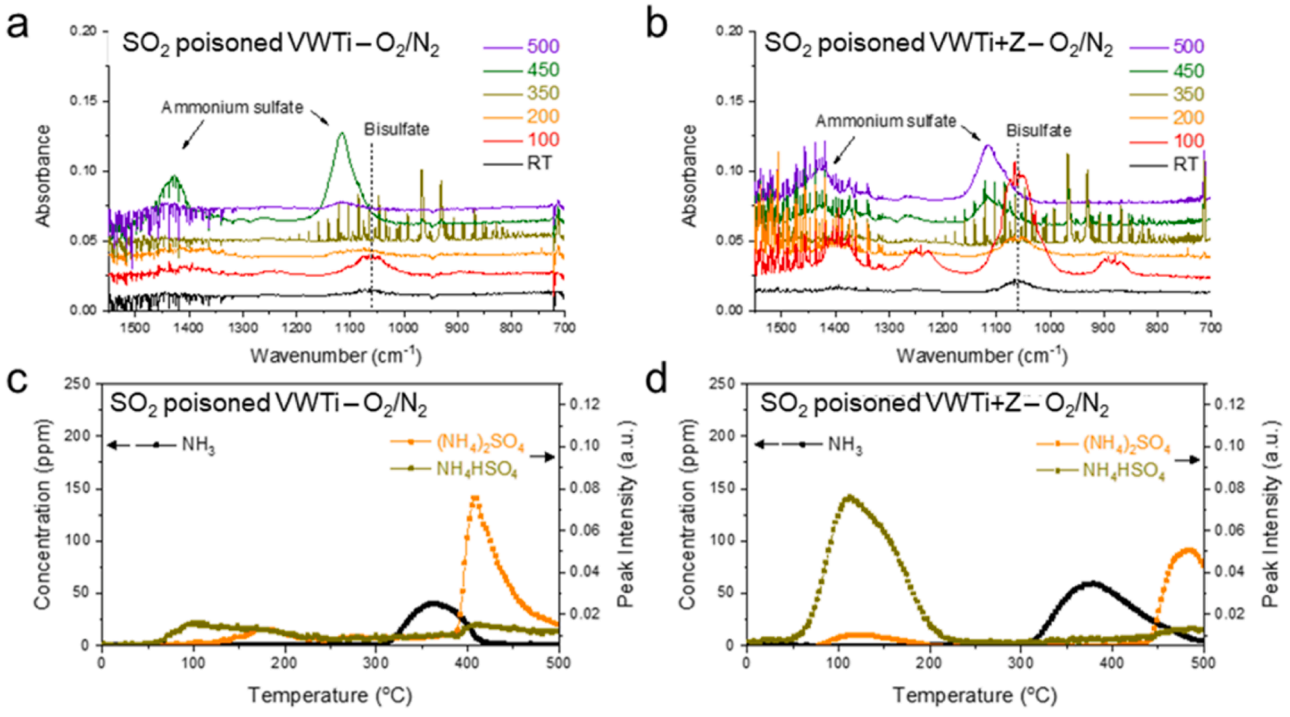

Fig. 4. Temperature-programmed decomposition-infrared spectroscopy results of sulfur-poisoned catalysts under air. (a, b) Raw Infrared spectra and (c, d) Concentration profiles of the gas species from sulfur poisoned VWTi and VWTi+Z catalysts, respectively during the decomposition under 20% O_2/N_2 conditions.

the vibrations of ammonium and bisulfate ions, respectively (Fig. S6a, b). As the temperature increased, the ammonium species were decomposed within 35 min (450 °C) (Fig. S6c), and the peak of the bisulfate species (1250 cm^{-1}) shifted to that of the sulfate species (1195 cm^{-1}) at 500 °C (Fig. S6a, b). Significantly, more abundant sulfate species were present on the catalyst surface under O_2/N_2 conditions than what was observed under N_2 conditions (Fig. S6d) thus indicating that the sulfate species are much more stable on the VWTi surface under oxidative

conditions, which leads to sulfur decomposition in the form of sulfates instead of sulfur dioxide. It was thus concluded that the presence of O_2 inhibits the reduction of sulfur from the S^{6+} (HSO_4^- or SO_4^{2-}) state to the S^{4+} (SO_2) state, which leads to the desorption of the sulfur species as an aerosol of the ammonium salt complex [29].

As the deposited sulfur species desorbed with the ammonium salt, the amount of the desorbed ammonia decreased in both VWTi and VWTi+Z under oxidative conditions compared with that under N_2 conditions (VWTi: from 0.132 to 0.043 mmol/g, VWTi+Z: from 0.185 to 0.094 mmol/g) (Figs. 3c, d and 4c, d). The differences in ammonia desorption were almost identical for VWTi and VWTi+Z (0.089 and 0.091 mmol/g, respectively), since the amount of the deposited ammonium (bi)sulfate species per gram of catalyst was the same in both catalysts (Table S1). The ammonium (bi)sulfate species in VWTi+Z were desorbed at a temperature (490 °C) higher than that in VWTi (405 °C) since the condensation effect of the micropore structure and the stabilization effect of the Al sites in the Y zeolite hinder their decomposition [30,44]. It is noteworthy that additional desorption peaks of ammonium bisulfate were observed at very low temperatures in the range of 100–200 °C Fig. 4a-d. These desorption peaks were observed for both the SO_2-poisoned VWTi and SO_2-poisoned VWTi+Z catalysts, and they were more intense in the SO_2-poisoned VWTi+Z catalyst. The intensity profiles of the ammonium bisulfate and the H_2O band (Fig. S7) demonstrated that the desorption of the ABS species occurs simultaneously with the desorption of water at 50 °C. The desorption of ABS at a low temperature can be attributed to the desorption of water which justifies why this phenomenon was more intensely observed in the VWTi+Z catalyst which adsorbed a much larger amount of water, as confirmed by the larger intensity of the water band (Fig. S7) and the dynamic vapor sorption analysis (Fig. S8). This is attributed to hydrophilicity of the physically mixed zeolite. Additionally, the desorption band of the bisulfate aerosol occurred even at 40 °C upon the exposure of the SO_2-poisoned VWTi catalyst to a dehydrated O_2/N_2 gas (Fig. S9) [45]. Based on these observations, it was concluded that water adsorbed in the catalyst can dissolve the deposited ABS, and the evaporation of the ABS-containing water causes the formation of the aerosol species.

To verify the amount of desorbed ABS at low temperatures, the change in the mass of SO_2-poisoned VWTi+Z was investigated by thermogravimetric analysis (TGA) under O_2/N_2 conditions. Although an ABS aerosol peak was observed at low temperatures in the IR spectra, the TGA profile of the SO_2-poisoned VWTi+Z catalyst did not exhibit any decrease in mass at these temperatures (< 200 °C) (Fig. S10). This discrepancy indicates that only a trace amount of ABS species can be desorbed at low temperatures, in contrast to the large desorption peak observed in the TPD-IR profiles. Consequently, the desorption at low temperature barely influences the total amount of residual sulfur, and we speculated that the IR intensity of the desorbed species was exaggerated compared to its actual amount (Fig. 4a-d) [45]. Investigating the decomposition behavior of ABS revealed two interesting findings. First, the sulfur species of the ABS deposited on the VWTi and VWTi+Z catalysts exhibits different behaviors depending on the gas conditions where it decomposes as SO_2 and (bi)sulfates with ammonium under inert (N_2) and oxidative (O_2/N_2) conditions, respectively. Second, the deposited ABS dissolves in adsorbed water on the catalyst surface at room temperature, as evidenced by the presence of ABS aerosol species in the decomposition profile. Although the desorption of ABS is not significant quantitatively, this phenomenon is a clear and significant qualitative evidence of ABS dissolution in the adsorbed water in the zeolite. Furthermore, ABS dissolution can be promoted by a larger amount of water as it provides a bigger amount of solvent for ABS to be dissolved.

3.3. Development of a new regeneration method

Although the physically mixed VWTi+Z catalyst demonstrated excellent sulfur resistance, its activity remained unstable probably due to the residual ABS on the active vanadia sites (Fig. S3). After understanding the properties of the catalyst and ABS (vide supra), a novel strategy for the regeneration of VWTi+Z catalyst was proposed to solve this issue. The proposed method is different from the typically employed thermal decomposition of accumulated ABS above 350 °C [30,44]. The results from various analyses demonstrated that water adsorbed in the catalyst can solvate the ABS molecules, and the presence of Y zeolite in the physically mixed catalyst promotes this solvation phenomenon due to its hydrophilic properties. Thus, a regeneration method was devised to expose the aged catalyst to wet conditions at ambient temperature in order to facilitate ABS solvation as follows:

i) After sulfur aging, the poisoned catalyst is purged under a 10% O_2/N_2 gas flow for 30 min at 220 °C.
ii) The poisoned catalyst is cooled to 30–40 °C under a 10% O_2/N_2 atmosphere.
iii) The catalyst is exposed to 3% H_2O under a 10% O_2/N_2 atmosphere at 30–40 °C for 1 h.
iv) The catalyst is exposed to a dehydrated gas (10% O_2/N_2) for 15 min, and the temperature is increased to 220 °C.

The main aim of this method is to saturate the catalyst with water at ambient temperature and maximize the solvation of ABS into the zeolite. The water adsorbed on the zeolite facilitated the removal of residual ABS from the vanadia by attracting it to the zeolite domain and facilitated a recovery of the vanadia active sites. This new regeneration protocol was then applied to VWTi+Z and VWTi catalysts deactivated under standard SCR condition with 100 ppm SO_2 at 220 °C for 22 h. The NO_x conversion profile (Fig. 5a) clearly demonstrated that the SCR activity of the VWTi+Z catalyst deactivated by 12% after sulfur poisoning was almost completely recovered by two consecutive cycles of the proposed regeneration process. As expected, these results indicated that the proposed protocol is effective to recover a sulfur poisoned VWTi+Z catalyst.

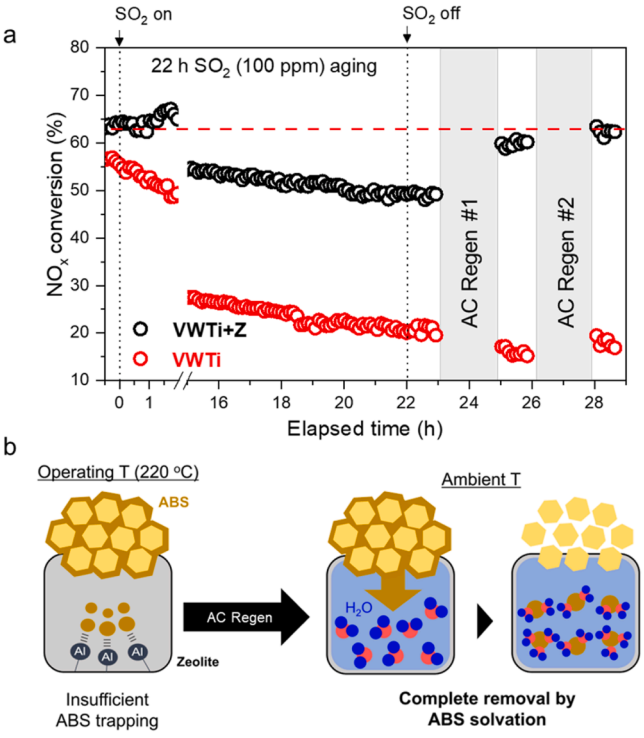

Fig. 5. (a) A result of ambient temperature regeneration on sulfur-poisoned catalysts. NO_x conversion profiles during sulfur poisoning under SCR condition (500 ppm NO_x, 600 ppm NH_3, 10% O_2, 5% CO_2 and 10% H_2O) with 100 ppm SO_2 at 220 °C, and AC Regen over the VWTi+Z and VWTi catalysts. (b) The schematic shows AC Regen process.

However, this method had a little effect on the deactivated VWTi catalyst, thus indicating that a physically mixed zeolite is essential to enable this regeneration approach. It is important to point out that the regeneration occurred at an ambient temperature under humid air conditions, and consequently the process can be designated as an 'ambient condition regeneration' (AC Regen) process.

The data in Fig. S11 show that the presence of a residual amount of sulfur after the regeneration. The result indicates that this regeneration protocol did not decompose the sulfur species, but it is more likely to change the spatial distribution of ABS. We propose that liquid water adsorbed in the zeolite solvated the ABS molecules, facilitated their migration into the zeolite and eventually liberated vanadia active sites, which is annotated as the "solvation" of ABS (Fig. 5b). This phenomenon is attributed to the disparity of the water content in the two physically mixed materials, vanadia-titania and the Y zeolite. A larger amount of water in the Y zeolite than in vanadia-titania results in a different chemical potential of ABS in the adsorbed water at vanadia-titania and zeolite. The 3 vol% of water corresponds to a 40% relative humidity at 40 °C, and it indicates that a 10-fold larger amount of water is adsorbed in zeolite per gram compared with vanadia-titania (Fig. S8). The mass ratio of vanadia-titania to zeolite is 2:1, so the total amount of adsorbed water would be 5 times larger in zeolite than in vanadia-titania. Simply assuming twice larger amount of sulfur in the zeolite (as the physically mixed zeolite reduces the deactivation rate of vanadia-titania by 1/3), the chemical potential of ABS is 2.5 times higher in vanadia-titania compared to zeolite when the sulfur-aged catalyst is treated under humid air (3 vol% of water) at ambient temperature. Here, the water cannot migrate due to the relatively less hydrophilic vanadia-titania, so ABS migrates form vanadia-titania to the zeolite to compensate the different chemical potential. The interface of the two physically mixed domains functions like a "salt bridge", allowing the ionic salt (ABS) to pass through and preventing the migration of water.

We estimate the maximum amount of ABS that Y zeolite in VWTi+Z can accommodate. As shown in Table S1, the sulfur aging under SCR conditions with 30 ppm of SO_2 at 220 °C for 22 h resulted in 0.45 wt% of sulfur deposition (1.6 wt% of ABS). Assuming that most of sulfur species is present on Y zeolite, this corresponds to 1.36 wt% of sulfur on a gram of Y zeolite (4.89 wt% of ABS). Since ABS was stabilized as a liquid phase or solution in the zeolite at the reaction temperature (220 °C), ABS migration led to pore filling of micropores in Y zeolite. Micropore volume distribution of VWTi+Z shown in Fig. S12 demonstrates that 15% of micropore in Y zeolite is occupied by 4.89 wt% of ABS in the zeolite. Based on this volumetric occupancy of ABS in the zeolite, we surmise that the maximum capacity of Y zeolite for ABS would be 6.6 times what we experimentally observed, which is 32.6 wt % of ABS on the zeolite.

3.4. Investigation on effect of water

To investigate the effect of water, an AC Regen process was performed without the introduction of water in step iii) (Fig. 6). In comparison with almost complete regeneration in the AC Regen (with water), the activity of the VWTi+Z catalyst was barely restored after AC Regen without the presence of water. The results clearly evidence that the presence of water is essential for activating the AC Regen process. The effectiveness of the AC Regen protocol in a hydrophobic Y zeolite was also investigated. A hydrophobic Y zeolite was synthesized by functionalizing the surface hydroxyl groups with hydrocarbons using octadecyltrichlorosilane (OTS). The contact angle of the water droplets on the functionalized zeolite (OTS-Z) was approximately 135°, thus confirming that the surface of the zeolite is highly hydrophobic (Fig. 7a). By evaluating the sulfur resistance of the physically mixed VWTi+OTS-Z catalyst, a 14% decrease in the NO_x conversion (from 44% to 30%) was observed, which is almost the same as that of the VWTi+Z catalyst (Figs. 5 and 7b). However, in contrast to the completely regenerated VWTi+Z catalyst, only 28% of the initial SCR activity of the sulfur-

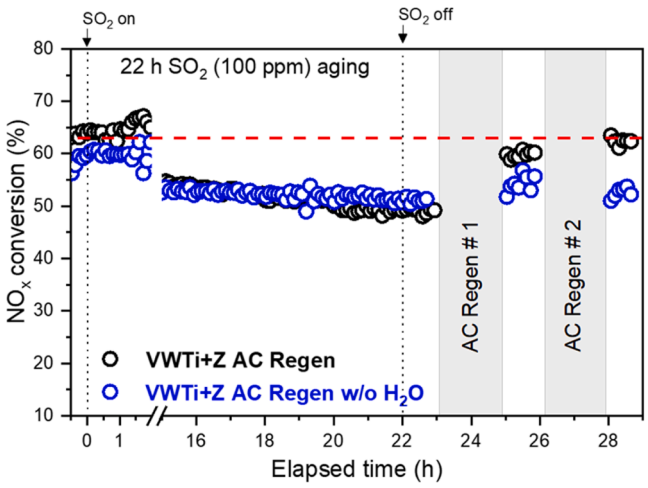

Fig. 6. Results of ambient temperature regeneration on VWTi+Z catalyst in the presence and absence of H_2O. NO_x conversion profile of the VWTi+Z catalyst with time-on-stream during SO_2 aging and following the AC Regen with H_2O (black) and without H_2O (blue). The reaction was performed under 500 ppm NO, 600 ppm NH_3, 10% O_2, 5% CO_2, 5% H_2O, 100 ppm SO_2 (when used) and N_2 balance.

poisoned VWTi+OTS-Z catalyst was recovered after AC Regen (Fig. 7b). The hydrophobic functional group in the OTS-Y zeolite must result in much less amount of water than pristine Y zeolite, which represents a weaker driving force to attract ABS into the zeolite regime. It was thus concluded that liquid water adsorbed in a zeolite is essential for activating the AC Regen process.

We have previously proposed an ABS migration behavior known as the "trapping" of ABS from vanadia to zeolite in a physically mixed VWTi+Z catalyst [30]. Owing to this trapping effect, the VWTi+Z catalyst exhibited a decrease of 15% only in NO_x conversion after 22 h aging with 100 ppm of sulfur despite the 40% decrease in that of VWTi, which represents high sulfur resistance of the physically mixed catalyst (Fig. 5). Likewise, data shown in Fig. 7 demonstrates that the VWTi+OTS-Z catalyst exhibits almost the same level of sulfur resistance with only a 15% decrease in NO_x conversion. This result demonstrates that the hydrophobic surface with the organic functional groups does not influence the ABS 'trapping' process from vanadia titania to zeolite, thus indicating that the migration of ABS from vanadia into the zeolite is facile at 220 °C. However, the ABS "solvation" process was dramatically deterred by the hydrophobic functionalization, and consequently it degraded the performance of the AC Regen process (Fig. 7). This discrepancy demonstrates that the two ABS migration processes, trapping and solvation, have fundamentally different mechanisms, particularly in terms of water participation. According to the results of our previous study, the trapping of ABS occurs at an operating temperature of NH_3-SCR (220 °C) where ABS exists as a liquid [30]. The migration of the liquid ABS via trapping is facilitated by the electrostatic interaction between the Al sites in zeolite and ABS, thus the trapping ability of zeolites is closely related to the amount of tetrahedral Al sites. Since water did not participate in this trapping process, the hydrophobic coating on the zeolite did not affect the sulfur resistance at 220 °C, in other word, the ability of ABS trapping (Fig. 7). However, ABS exists as a solid phase at ambient temperature where the AC Regen is performed. In the AC Regen, the migration of ABS occurs by the solvation process. The most significant driving force in this process is the different chemical potential of ABS derived by the different water content in vanadia-titania and zeolite. Therefore, the hydrophobic coating on the zeolite seriously deteriorates the AC Regen process. The thermodynamic stabilization effect by solvation of the ABS molecules acts as a much stronger driving force than ABS trapping, thus, the AC Regen process results in a complete migration of the ABS to the zeolite and full restoration of the catalytic

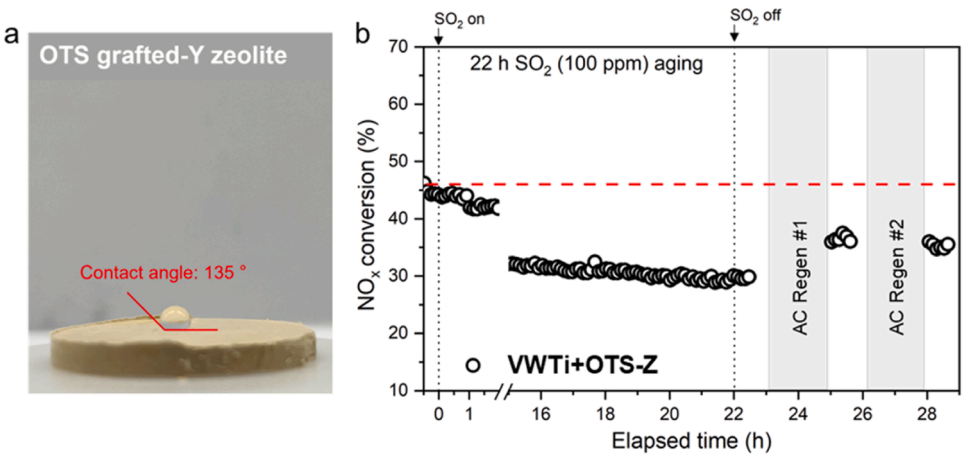

Fig. 7. (a) Contact angle of water drop on the surface to show hydrophobicity of OTS grafted Y zeolite (OTS-Z). (b) NO_x conversion profile with time-on-stream during SO_2 aging and following the AC Regen in the VWTi+OTS-Z catalyst. The reaction was performed under 500 ppm NO, 600 ppm NH_3, 10% O_2, 5% CO_2, 10% H_2O, 100 ppm SO_2 (when used) and N_2 balance.

activity.

4. Conclusion

this study proposes an innovative and unprecedent protocol for catalyst regeneration to prolong its lifetime. The sulfur aged VWTi+Z catalyst was successfully regenerated by the AC Regen process devised based on rigorous investigations on the sulfur species on the catalyst. The proposed regeneration protocol is facilitated by solvating the ABS into liquid water adsorbed in a zeolite at ambient temperature. It is noteworthy that none of followings is necessary in this protocol; i) thermal treatment at high temperatures above operating temperature (220 °C) which is typically used in conventional regeneration method, ii) additional chemicals other than the reactants, nor iii) the retrieval of the used catalyst from the reactor. The proposed protocol only requires a flow of air containing 3% of water over the sulfur poisoned VWTi+Z catalyst at ambient temperature. From a practical perspective, this process does not consume any additional energy or cost to regenerate the catalyst. Consequently, is a clean and energy-efficient strategy. As this protocol does not decompose ABS, but just redistributes it to zeolite, conventional regeneration would be necessary to decompose ABS when the zeolite is fully saturated in the end. Nevertheless, a devised regeneration method can dramatically reduce the frequency of such a decomposition process by prolonging the lifetime of the catalyst without any cost.

CRediT authorship contribution statement

Hwangho Lee: Conceptualization, Analysis, Writing – original draft. **Inhak Song:** Investigation, Writing – review & editing. **Se Won Jeon:** Writing – review & editing. **Keon Ha Hwang:** Investigation, Writing – review & editing. **Do Heui Kim:** Conceptualization, Supervision, Funding acquisition.

Declaration of Competing Interest

The authors declare that they have no known competing financial interests or personal relationships that could have appeared to influence the work reported in this paper.

Data availability

Data will be made available on request.

Acknowledgments

This research was supported by the Basic Science Research Program administered by the National Research Foundation of Korea (NRF) with funding provided by the Ministry of Science, ICT & Future Planning (MSIP) (grant numbers NRF-2016R1A5A1009592 and NRF-2022R1A2C3013253).

Appendix A. Supporting information

Supplementary data associated with this article can be found in the online version at doi:10.1016/j.apcatb.2023.123333.

References

[1] R. York, S.E. Bell, Energy transitions or additions? Energy Res. Soc. Sci. 51 (2019) 40–43.
[2] U. Asghar, S. Rafiq, A. Anwar, T. Iqbal, A. Ahmed, F. Jamil, M.S. Khurram, M. M. Akbar, A. Farooq, N.S. Shah, Y.-K. Park, Review on the progress in emission control technologies for the abatement of CO_2, SOx and NOx from fuel combustion, J. Environ. Chem. Eng. 9 (2021), 106064.
[3] J.E. Jonson, J. Borken-Kleefeld, D. Simpson, A. Nyíri, M. Posch, C. Heyes, Impact of excess NOx emissions from diesel cars on air quality, public health and eutrophication in Europe, Environ. Res. Lett. 12 (2017), 094017.
[4] G.P. Chossière, R. Malina, A. Ashok, I.C. Dedoussi, S.D. Eastham, R.L. Speth, S.R. H. Barrett, Public health impacts of excess NOx emissions from Volkswagen diesel passenger vehicles in Germany, Environ. Res. Lett. 12 (2017), 034014.
[5] S.C. Anenberg, J. Miller, R. Minjares, L. Du, D.K. Henze, F. Lacey, C.S. Malley, L. Emberson, V. Franco, Z. Klimont, C. Heyes, Impacts and mitigation of excess diesel-related NOx emissions in 11 major vehicle markets, Nature 545 (2017) 467–471.
[6] C.K. Lambert, Perspective on SCR NOx control for diesel vehicles, React. Chem. Eng. 4 (2019) 969–974.
[7] M.D. Amiridis, I.E. Wachs, G. Deo, J.-M. Jehng, Reactivity of V2O5 catalysts for the selective catalytic reduction of NO by NH3: influence of vanadia loading, H2O, and SO2, J. Catal. 161 (1996) 247–253.
[8] I.E. Wachs, G. Deo, B.M. Weckhuysen, A. Andreini, M.A. Vuurman, M. de Boer, M. D. Amiridis, Selective catalytic reduction of NO with NH3 over supported vanadia catalysts, J. Catal. 161 (1996) 211–221.
[9] A.M. Beale, F. Gao, I. Lezcano-Gonzalez, C.H. Peden, J. Szanyi, Recent advances in automotive catalysis for NOx emission control by small-pore microporous materials, Chem. Soc. Rev. 44 (2015) 7371–7405.
[10] J.H. Kwak, R.G. Tonkyn, D.H. Kim, J. Szanyi, C.H. Peden, Excellent activity and selectivity of Cu-SSZ-13 in the selective catalytic reduction of NOx with NH3, J. Catal. 275 (2010) 187–190.
[11] C. Paolucci, I. Khurana, A.A. Parekh, S. Li, A.J. Shih, H. Li, J.R. Di Iorio, J. D. Albarracin-Caballero, A. Yezerets, J.T. Miller, Dynamic multinuclear sites formed by mobilized copper ions in NOx selective catalytic reduction, Science 357 (2017) 898–903.
[12] N.-Y. Topsøe, Mechanism of the selective catalytic reduction of nitric oxide by ammonia elucidated by in situ on-line Fourier transform infrared spectroscopy, Science 265 (1994) 1217–1219.

[13] G.T. Went, L.-J. Leu, R.R. Rosin, A.T. Bell, The effects of structure on the catalytic activity and selectivity of V2O5/TiO2 for the reduction of NO by NH3, J. Catal. 134 (1992) 492–505.
[14] Y.J. Kim, J.K. Lee, K.M. Min, S.B. Hong, I.-S. Nam, B.K. Cho, Hydrothermal stability of CuSSZ13 for reducing NOx by NH3, J. Catal. 311 (2014) 447–457.
[15] M. Zhu, J.K. Lai, U. Tumuluri, Z. Wu, I.E. Wachs, Nature of active sites and surface intermediates during SCR of NO with NH3 by supported V2O5-WO3/TiO2 catalysts, J. Am. Chem. Soc. 139 (2017) 15624–15627.
[16] A. Marberger, D. Ferri, M. Elsener, O. Krocher, The significance of Lewis acid sites for the selective catalytic reduction of nitric oxide on vanadium-based catalysts, Angew. Chem. Int. Ed. Engl. 55 (2016) 11989–11994.
[17] W. Hu, T. Selleri, F. Gramigni, E. Fenes, K.R. Rout, S. Liu, I. Nova, D. Chen, X. Gao, E. Tronconi, On the redox mechanism of low-temperature NH3-SCR over Cu-CHA: a combined experimental and theoretical study of the reduction half cycle, Angew. Chem. Int. Ed. Engl. 133 (2021) 7273–7280.
[18] P.G. Smirniotis, D.A. Peña, B.S. Uphade, Low-temperature selective catalytic reduction (SCR) of NO with NH3 by using Mn, Cr, and Cu oxides supported on hombikat TiO2, Angew. Chem. Int. Ed. 40 (2001) 2479–2482.
[19] H.H. Phil, M.P. Reddy, P.A. Kumar, L.K. Ju, J.S. Hyo, SO2 resistant antimony promoted V2O5/TiO2 catalyst for NH3-SCR of NOx at low temperatures, Appl. Catal. B Environ. 78 (2008) 301–308.
[20] S.S.R. Putluru, L. Schill, A.D. Jensen, B. Siret, F. Tabaries, R. Fehrmann, Mn/TiO2 and Mn–Fe/TiO2 catalysts synthesized by deposition precipitation—promising for selective catalytic reduction of NO with NH3 at low temperatures, Appl. Catal. B Environ. 165 (2015) 628–635.
[21] S. Cimino, L. Lisi, M. Tortorelli, Low temperature SCR on supported MnOx catalysts for marine exhaust gas cleaning: Effect of KCl poisoning, Chem. Eng. J. 283 (2016) 223–230.
[22] Z. Liu, G. Sun, C. Chen, K. Sun, L. Zeng, L. Yang, Y. Chen, W. Wang, B. Liu, Y. Lu, Y. Pan, Y. Liu, C. Liu, Fe-doped Mn3O4 spinel nanoparticles with highly exposed Feoct–O–Mntet sites for efficient selective catalytic reduction (SCR) of NO with ammonia at low temperatures, ACS Catal. 10 (2020) 6803–6809.
[23] I. Song, H. Lee, S.W. Jeon, D.H. Kim, Controlling catalytic selectivity mediated by stabilization of reactive intermediates in small-pore environments: a study of Mn/TiO2 in the NH3-SCR reaction, ACS Catal. 10 (2020) 12017–12030.
[24] T. Ryu, S.B. Hong, Iron-exchanged UZM-35: an active NH3-SCR catalyst at low temperatures, Appl. Catal. B Environ. 266 (2020), 118622.
[25] Z. Lian, J. Wei, W. Shan, Y. Yu, P.M. Radjenovic, H. Zhang, G. He, F. Liu, J.F. Li, Z. Q. Tian, H. He, Adsorption-induced active vanadium species facilitate excellent performance in low-temperature catalytic NOx abatement, J. Am. Chem. Soc. 143 (2021) 10454–10461.
[26] P. Forzatti, I. Nova, E. Tronconi, Enhanced NH3 selective catalytic reduction for NOx abatement, Angew. Chem. Int. Ed. Engl. 48 (2009) 8366–8368.
[27] N.R. Jaegers, J.K. Lai, Y. He, E. Walter, D.A. Dixon, M. Vasiliu, Y. Chen, C. Wang, M.Y. Hu, K.T. Mueller, I.E. Wachs, Y. Wang, J.Z. Hu, Mechanism by which tungsten oxide promotes the activity of supported V2O5/TiO2 catalysts for NOx abatement: structural effects revealed by 51V MAS NMR spectroscopy, Angew. Chem. Int Ed. Engl. 58 (2019) 12609–12616.
[28] Y. Jangjou, Q. Do, Y. Gu, L.-G. Lim, H. Sun, D. Wang, A. Kumar, J. Li, L.C. Grabow, W.S. Epling, Nature of Cu active centers in Cu-SSZ-13 and their responses to SO2 exposure, ACS Catal. 8 (2018) 1325–1337.
[29] K. Guo, J. Ji, W. Song, J. Sun, C. Tang, L. Dong, Conquering ammonium bisulfate poison over low-temperature NH3-SCR catalysts: a critical review, Appl. Catal. B Environ. 297 (2021), 120388.
[30] I. Song, H. Lee, S.W. Jeon, I.A.M. Ibrahim, J. Kim, Y. Byun, D.J. Koh, J.W. Han, D. H. Kim, Simple physical mixing of zeolite prevents sulfur deactivation of vanadia catalysts for NOx removal, Nat. Commun. 12 (2021) 901.
[31] S.W. Jeon, I. Song, H. Lee, J. Kim, Y. Byun, D.J. Koh, D.H. Kim, Enhanced SO2 resistance of V2O5/WO3-TiO2 catalyst physically mixed with alumina for the selective catalytic reduction of NOx with NH3, Chem. Eng. J. 433 (2022), 133836.
[32] I. Song, S.W. Jeon, H. Lee, D.H. Kim, Tailoring the mechanochemical interaction between vanadium oxides and zeolite for sulfur-resistant DeNO catalysts, Appl. Catal. B Environ. 316 (2022), 121672.
[33] Y. Chen, C. Li, J. Chen, X. Tang, Self-prevention of well-defined-facet Fe2O3/MoO3 against deposition of ammonium bisulfate in low-temperature NH3-SCR, Environ. Sci. Technol. 52 (2018) 11796–11802.
[34] X. Wang, X. Du, L. Zhang, Y. Chen, G. Yang, J. Ran, Promotion of NH4HSO4 decomposition in NO/NO2 contained atmosphere at low temperature over V2O5-WO3/TiO2 catalyst for NO reduction, Appl. Catal. A Gen. 559 (2018) 112–121.
[35] X. Wang, X. Du, S. Liu, G. Yang, Y. Chen, L. Zhang, X. Tu, Understanding the deposition and reaction mechanism of ammonium bisulfate on a vanadia SCR catalyst: a combined DFT and experimental study, Appl. Catal. B Environ. 260 (2020), 118168.
[36] Y. Cao, F. Han, M. Wang, L. Han, C. Zhang, J. Wang, W. Bao, L. Chang, Regeneration of the waste selective catalytic reduction denitrification catalyst by nitric acid washing, ACS Omega 4 (2019) 16629–16637.
[37] S.T. Choo, S.D. Yim, I.-S. Nam, S.-W. Ham, J.-B. Lee, Effect of promoters including WO3 and BaO on the activity and durability of V2O5/sulfated TiO2 catalyst for NO reduction by NH3, Appl. Catal. B Environ. 44 (2003) 237–252.
[38] Y. Xi, N.A. Ottinger, Z.G. Liu, New insights into sulfur poisoning on a vanadia SCR catalyst under simulated diesel engine operating conditions, Appl. Catal. B Environ. 160–161 (2014) 1–9.
[39] C. Li, M. Shen, T. Yu, J. Wang, J. Wang, Y. Zhai, The mechanism of ammonium bisulfate formation and decomposition over V/WTi catalysts for NH3-selective catalytic reduction at various temperatures, Phys. Chem. Chem. Phys. 19 (2017) 15194–15206.
[40] J.R. Di Iorio, S.A. Bates, A.A. Verma, W.N. Delgass, F.H. Ribeiro, J.T. Miller, R. Gounder, The dynamic nature of brønsted acid sites in Cu–zeolites during NOx selective catalytic reduction: quantification by gas-phase ammonia titration, Top. Catal. 58 (2015) 424–434.
[41] J. Luo, F. Gao, K. Kamasamudram, N. Currier, C.H. Peden, A. Yezerets, New insights into Cu/SSZ-13 SCR catalyst acidity. Part I: Nature of acidic sites probed by NH3 titration, J. Catal. 348 (2017) 291–299.
[42] K.D. Beyer, J. Bothe, Ammonium bisulfate/water: a pseudobinary system, J. Phys. Chem. A 110 (2006) 7105–7112.
[43] M. Hallquist, D.J. Stewart, S.K. Stephenson, R. Anthony Cox, Hydrolysis of N2O5 on sub-micron sulfate aerosols, Phys. Chem. Chem. Phys. 5 (2003) 3453–3463.
[44] K. Guo, G. Fan, D. Gu, S. Yu, K. Ma, A. Liu, W. Tan, J. Wang, X. Du, W. Zou, C. Tang, L. Dong, Pore size expansion accelerates ammonium bisulfate decomposition for improved sulfur resistance in low-temperature NH3-SCR, ACS Appl. Mater. Interfaces 11 (2019) 4900–4907.
[45] I. Tang, H. Munkelwitz, Aerosol growth studies—III ammonium bisulfate aerosols in a moist atmosphere, J. Aerosol Sci. 8 (1977) 321–330.